

Fermilab

SDC SOLENOID DESIGN NOTE #135

TITLE: Calculation of Radiation Thickness of Carbon Fiber-Epoxy Composite

AUTHOR: *Ron Fast*
Ron Fast

DATE: February 22, 1991

ABSTRACT: I calculated the radiation thickness of CFRP as about 280 mm.

REFERENCE: "Review of Particle Properties," Physics Letters B, Vol. 239, 12 April 1990, Table III.5 (copy attached).

NOMENCLATURE

I realize that I use "CFRP" (carbon fiber reinforced plastic), "carbon (or graphite)-epoxy composite", and "epoxy-carbon composite" interchangeably. Please forgive my inconsistency.

METHODOLOGY

The above reference says that "the radiation length in a mixture or compound, may be approximated by

$$1/X_0 = \sum(f_i/X_i)$$

where f_i and X_i are the fraction by weight and radiation length for the i th element."

Table III.5 gives the radiation length X_0 (density) in g/cm^2 for glass (SiO_2) and for G-10 epoxy-glass composite. Using these two values I used the above equation to calculate X_0 for epoxy. With that value and the X_0 for carbon, I derived X_0 for epoxy-carbon composite.

CALCULATION OF X_0 FOR EPOXY

From Table III.5, $X(\text{glass, SiO}_2) = 27.05 \text{ g/cm}^2$ and $X(\text{G-10, 60\% SiO}_2, 40\% \text{ epoxy}) = 33.0 \text{ g/cm}^2$.

Assuming that those fractions are weight percent,

$$1/X(\text{G-10}) = 0.6/X(\text{glass}) + 0.4/X(\text{epoxy})$$

and

$$\begin{aligned} X(\text{epoxy}) &= 0.4/[1/X(\text{G-10}) - 0.6/X(\text{glass})] \\ &= 0.4/[1/33.0 - 0.6/27.05] \end{aligned}$$

and

$$X(\text{epoxy}) = 49.25 \text{ g/cm}^2.$$

CALCULATION OF X_0 FOR EPOXY-CARBON COMPOSITE

$X_0(\text{carbon}) = 42.7 \text{ g/cm}^2$; assuming 60 w/o carbon and 40 w/o epoxy,

$$1/X_0(\text{CFRP}) = 0.6/42.7 + 0.4/49.25$$

and

$$X_0(\text{CFRP}) = 45.10 \text{ g/cm}^2.$$

The "Advanced Composite Materials Handbook" gives the typical density of graphite-epoxy composite as 1.6 g/cm^3 . Using this value,

$$X_0(\text{CFRP}) = 282 \text{ mm.}$$

For 70 w/o carbon and 30 w/o epoxy,

$$X_0(\text{CFRP}) = 278 \text{ mm.}$$

These values are quite a bit smaller than the value given by Green for filament-wound composite (350 mm) [1]. They are slightly larger than the value given by Wake for the graphite cloth-epoxy shell for the Venus solenoid (240 mm) [2].

CONCLUSION

For the moment, we should probably use 280 mm as the radiation thickness of CFRP. When SCI gives me the weight fractions and the density of the CFRP cylinder they are designing I will recalculate X_0 .

OTHER REFERENCES

[1] M.A. Green, "PEP Detector Magnet: Large Thin Solenoid Magnet Cryostat: The Design of Minimum Radiation Length Vacuum Vessels," LBL Engineering Note AB0103-M5009 (Dec 23, 1976).

[2] M. Wake, CFRP vacuum chamber for a large superconducting magnet, in: "Proceedings of the 6th KEK Vacuum Conference," KEK, Japan.

M. GERARDI
ISSN 0370-2693

PHYSICS LETTERS B

VOLUME 239

12 APRIL 1990

PYLBAJ 239, 1-516 (1990)

REVIEW OF PARTICLE PROPERTIES

Particle Data Group



NORTH-HOLLAND

ATOMIC AND NUCLEAR PROPERTIES OF MATERIALS*

Material	Z	A	Nuclear ^a total cross section σ_T [barn]	Nuclear ^b inelastic cross section σ_I [barn]	Nuclear ^c collision length λ_T [g/cm ²]	Nuclear ^c interaction length λ_I [g/cm ²]	$\frac{dE}{dx} _{\min}$ ^d [MeV] [g/cm ²]	Radiation length ^e		Density ^f [g/cm ³] () is for gas [g/l]	Refractive index n^f () is $(n-1) \times 10^6$ for gas
								X_0 [g/cm ²] () is for gas	[cm]		
H ₂	1	1.01	0.0387	0.033	43.3	50.8	4.12	61.28	865	0.0708(0.090)	1.112(140)
D ₂	1	2.01	0.073	0.061	45.7	54.7	2.07	122.6	757	0.162(0.177)	1.128
He	2	4.00	0.133	0.102	49.9	65.1	1.94	94.32	755	0.125(0.178)	1.024(35)
Li	3	6.94	0.211	0.157	54.6	73.4	1.58	82.76	155	0.534	—
Be	4	9.01	0.268	0.199	55.8	75.2	1.61	65.19	35.3	1.848	—
C	6	12.01	0.331	0.231	60.2	86.3	1.78	42.70	18.8	2.265 ^g	—
N ₂	7	14.01	0.379	0.265	61.4	87.8	1.82	37.99	47.0	0.808(1.25)	1.205(300)
O ₂	8	16.00	0.420	0.292	63.2	91.0	1.82	34.24	30.0	1.14(1.43)	1.22(266)
Ne	10	20.18	0.507	0.347	66.1	96.6	1.73	28.94	24.0	1.207(0.90)	1.092(67)
Al	13	26.98	0.634	0.421	70.6	106.4	1.62	24.01	8.9	2.70	—
Si	14	28.09	0.660	0.440	70.6	106.0	1.66	21.82	9.36	2.33	—
Ar	18	39.95	0.868	0.566	76.4	117.2	1.51	19.55	14.0	1.40(1.78)	1.233(283)
Ti	22	47.88	0.995	0.637	79.9	124.9	1.51	16.17	3.56	4.54	—
Fe	26	55.85	1.120	0.703	82.8	131.9	1.48	13.84	1.76	7.87	—
Cu	29	63.55	1.232	0.782	85.6	134.9	1.44	12.86	1.43	8.96	—
Ge	32	72.59	1.365	0.858	88.3	140.5	1.40	12.25	2.30	5.323	—
Sn	50	118.69	1.967	1.21	100.2	163	1.26	8.82	1.21	7.31	—
Xe	54	131.29	2.120	1.29	102.8	169	1.24	8.48	2.77	3.057(5.89)	(705)
W	74	183.85	2.767	1.65	110.3	185	1.16	6.76	0.35	19.3	—
Pt	78	195.08	2.861	1.708	113.3	189.7	1.15	6.54	0.305	21.45	—
Pb	82	207.19	2.960	1.77	116.2	194	1.13	6.37	0.56	11.35	—
U	92	238.03	3.378	1.98	117.0	199	1.09	6.00	≈0.32	≈18.95	—
Air, 20°C, 1 atm. (STP in paren.)					62.0	90.0	1.82	36.66	(30420)	0.001205(1.29)	1.000273(293)
H ₂ O					60.1	84.9	2.03	36.08	36.1	1.00	1.33
Shielding concrete ^h					67.4	99.9	1.70	26.7	10.7	2.5	—
SiO ₂ (quartz)					67.0	99.2	1.72	27.05	12.3	2.64	1.458
H ₂ (bubble chamber 26°K)					43.3	50.8	4.12	61.28	≈1000	≈0.063 ⁱ	1.100
D ₂ (bubble chamber 31°K)					45.7	54.7	2.07	122.6	≈900	≈0.140 ⁱ	1.110
H-Ne mixture (50 mole percent) ^j					65.0	94.5	1.84	29.70	73.0	0.407	1.092
Iford emulsion G5					82.0	134	1.44	11.0	2.89	3.815	—
NaI					94.8	152	1.32	9.49	2.59	3.67	1.775
BaF ₂					92.1	146	1.35	9.91	2.05	4.89	1.56
BGO (Bi ₄ Ge ₃ O ₁₂)					97.4	156	1.27	7.98	1.12	7.1	2.15
Polystyrene, scintillator (CH) ^k					58.4	82.0	1.95	43.8	42.4	1.032	1.581
Lucite, Plexiglas (C ₅ H ₈ O ₂)					59.2	83.6	1.95	40.55	≈34.4	1.16-1.20	≈1.49
Polyethylene (CH ₂)					56.9	78.8	2.09	44.8	≈47.9	0.92-0.95	—
Mylar (C ₅ H ₄ O ₂)					60.2	85.7	1.86	39.95	28.7	1.39	—
Borosilicate glass (Pyrex) ^l					66.2	97.6	1.72	28.3	12.7	2.23	1.474
CO ₂					62.4	90.5	1.82	36.2	(18310)	(1.977)	(410)
Ethane C ₂ H ₆					55.73	75.71	2.25	45.66	(34035)	0.509(1.356) ^m	(1.038) ^m
Methane CH ₄					54.7	74.0	2.41	46.5	(64850)	0.423(0.717)	(444)
Isobutane C ₄ H ₁₀					56.3	77.4	2.22	45.2	(16930)	(2.67)	(1270)
NaF					66.78	97.57	1.69	29.87	11.68	2.558	1.336
LiF					62.00	88.24	1.66	39.25	14.91	2.632	1.392
Freon 12 (CCl ₂ F ₂) gas, 26°C, 1 atm. ⁿ					70.6	106	1.62	23.7	4810	(4.93)	1.001080
Silica Aerogel ^o					65.5	95.7	1.83	29.85	≈150	0.1-0.3	1.0+0.25ρ
NEMA G10 plate ^p					62.6	90.2	1.87	33.0	19.4	1.7	—

ATOMIC AND NUCLEAR PROPERTIES OF MATERIALS (Cont'd)

Material	Dielectric constant ($\kappa = \epsilon/\epsilon_0$) () is $(\kappa-1) \times 10^6$ for gas	Young's modulus [10^6 psi]	Coeff. of thermal expansion [10^{-6} cm/cm-°C]	Specific heat [cal/g-°C]	Electrical resistivity [$\mu\Omega$ cm(@°C)]	Thermal conductivity [cal/cm-°C-sec]
H ₂	(253.9)	—	—	—	—	—
He	(64)	—	—	—	—	—
Li	—	—	56	0.86	8.55(0°)	0.17
Be	—	37	12.4	0.436	5.885(0°)	0.38
C	—	0.7	0.6-4.3	0.165	1375(0°)	0.057
N ₂	(548.5)	—	—	—	—	—
O ₂	(495)	—	—	—	—	—
Ne	(127)	—	—	—	—	—
Al	—	10	23.9	0.215	2.65(20°)	0.53
Si	11.9	16	2.8-7.3	0.162	—	0.20
Ar	(517)	—	—	—	—	—
Ti	—	16.8	8.5	0.126	50(0°)	—
Fe	—	28.5	11.7	0.11	9.71(20°)	0.18
Cu	—	16	16.5	0.092	1.67(20°)	0.94
Ge	16.0	—	5.75	0.073	—	0.14
Sn	—	6	20	0.052	11.5(20°)	0.16
Xe	—	—	—	—	—	—
W	—	50	4.4	0.032	5.5(20°)	0.48
Pt	—	21	8.9	0.032	9.83(0°)	0.17
Pb	—	2.6	29.3	0.038	20.65(20°)	0.083
U	—	—	36.1	0.028	29(20°)	0.064

* Table revised April 1988 by R.W. Kenney. σ_T , σ_I , λ_T , and λ_I are energy dependent. Values quoted apply to high energy range given in footnote a or b, where energy dependence is weak.

- a. σ_{total} at 80-240 GeV for neutrons ($\approx \sigma$ for protons) from Murthy *et al.*, Nucl. Phys. B92, 269 (1975). This scales approximately as $A^{0.77}$.
- b. $\sigma_{inelastic} = \sigma_{total} - \sigma_{elastic} - \sigma_{quasielastic}$; for neutrons at 60-375 GeV from Roberts *et al.*, Nucl. Phys. B159, 56 (1979). For protons and other particles, see Carroll *et al.*, Phys. Lett. 80B, 319 (1979); note that $\sigma_I(p) \approx \sigma_I(n)$. σ_I scales approximately as $A^{0.71}$.
- c. Mean free path between collisions (λ_T) or inelastic interactions (λ_I), calculated from $\lambda = A/(N \times \sigma)$, where N is Avogadro's number.
- d. For minimum-ionizing protons and pions from Barkas and Berger, *Tables of Energy Losses and Ranges of Heavy Charged Particles*, NASA-SP-3013 (1964). For electrons and positrons see: M.J. Berger and S.M. Seltzer, *Stopping Powers and Ranges of Electrons and Positrons* (2nd Ed.), U.S. National Bureau of Standards report NBSIR 82-2550-A (1982).
- e. From Y.S. Tsai, Rev. Mod. Phys. 46, 815 (1974); X_0 data for all elements up to uranium may be found here. Corrections for molecular binding applied for H₂ and D₂. Parentheses refer to gaseous form at STP (0°C, 1 atm.).
- f. Values for solids, or the liquid phase at boiling point, except as noted. Values in parentheses for gaseous phase at STP (0°C, 1 atm.). Refractive index given for sodium D line.
- g. For pure graphite: industrial graphite density may vary 2.1-2.3 g/cm³.
- h. Standard shielding blocks, typical composition O₂ 52%, Si 32.5%, Ca 6%, Na 1.5%, Fe 2%, Al 4%, plus reinforcing iron bars. The attenuation length, $\ell = 115 \pm 5$ g/cm², is also valid for earth (typical $\rho = 2.15$), from CERN-LRL-RHEL Shielding exp., UCRL-17841 (1968).
- i. Density may vary about $\pm 3\%$, depending on operating conditions.
- j. Values for typical working conditions with H₂ target: 50 mole percent, 29°K, 7 atm.
- k. Typical scintillator: e.g., PILOT B and NE 102A have an atomic ratio H/C = 1.10.
- l. Main components: 80% SiO₂ + 12% B₂O₃ + 5% Na₂O.
- m. Solid ethane density at -60°C; gaseous refractive index at 0°C, 546 mm pressure.
- n. Used in Čerenkov counters. Values at 26°C and 1 atm. Indices of refraction from E.R. Hayes, R.A. Schluter, and A. Tamosaitis, ANL-6916 (1964).
- o. $n(\text{SiO}_2) + 2n(\text{H}_2\text{O})$ used in Čerenkov counters. ρ = density in g/cm³. From M. Cantin *et al.*, Nucl. Instr. and Meth. 118, 177 (1974).
- p. G10-plate, typical 60% SiO₂ and 40% epoxy.

ages exceed the appraisal of the energetic knock-on the mean local while essentially particle speeds.¹³ ngly sensitive to these effects. influenced by such

As a charged y small-angle omb scattering medium, hence omb scattering, ate to the total true Coulomb ory of Molière.¹⁵ (for below) it behaves ter probability on. A simpler s. is to use a rojected angular

(6)

), velocity. and the thickness of below). The angle particles with $\beta = 1 < x/X_0 < 100$. ological approach. F of the Molière accuracies of 2%

ng

(7)

ular distributions

(8)

(9)

ation. $\theta_{space}^2 \approx$

orthogonal to the

Deflections into

distributed.

used to describe

auxiliary quantities

(10)

ly only in the limit

atters. The random

ted in a correlated

and Monte Carlo

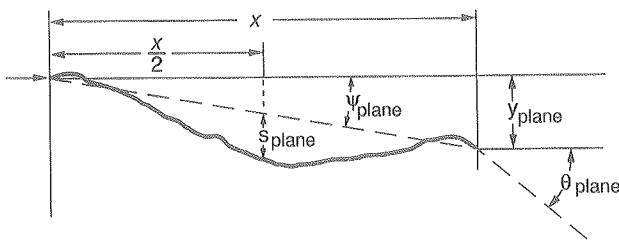


Fig. 1. Quantities useful in describing multiple Coulomb scattering. The particle is incident in the plane of the figure.

for the definition of the correlation coefficient). Obviously, $y \approx x\psi$. In addition, y and θ have correlation coefficient $\rho_{y\theta} = \sqrt{3}/2 \approx 0.87$. For Monte Carlo generation of a joint $(y_{plane}, \theta_{plane})$ distribution or for other calculations, it may be most convenient to work with independent Gaussian random variables (z_1, z_2) with mean zero and variance one and subsequently set

$$\begin{aligned}
 y_{plane} &= z_1 x \theta_0 (1 - \rho_{y\theta}^2)^{1/2} / \sqrt{3} + z_2 \rho_{y\theta} x \theta_0 / \sqrt{3} \\
 &= z_1 x \theta_0 / \sqrt{12} + z_2 x \theta_0 / 2; \\
 \theta_{plane} &= z_2 \theta_0.
 \end{aligned} \quad (11)$$

Note that the second term for y_{plane} equals $x\theta_{plane}/2$ and represents the displacement that would have occurred had the deflection θ_{plane} all occurred at the single point $x/2$.

(7) **Radiation length and associated quantities:** In dealing with electrons and photons at high energies, it is convenient to measure the thickness of the material in units of the radiation length X_0 . It is the mean distance over which a high-energy electron loses all but $1/e$ of its energy by bremsstrahlung, and in any case it is the appropriate scale length for describing high-energy electromagnetic cascades. X_0 is calculated and tabulated by Y.S. Tsai.¹⁸ His formula is less than straightforward, but can be approximated by¹⁹

$$X_0 = \frac{716.4 \text{ g cm}^{-2} A}{Z(Z+1) \ln(287/\sqrt{Z})}. \quad (12)$$

where Z is the atomic number and A the atomic weight of the medium. Results obtained with this formula agree with Tsai's values to better than 2.5% for all elements except helium, where the result is low by about 5%. The radiation length in a mixture or compound, may be approximated by

$$\frac{1}{X_0} = \sum \frac{f_i}{X_i}, \quad (13)$$

where f_i and X_i are the fraction by weight and radiation length for the i th element.

Radiative energy losses scale nearly proportionally to incident energy, while the dependence of ionization is only logarithmic. The energy at which the two are equal is called the *critical energy* E_c . For electrons it is given approximately by²⁰

$$E_c = \frac{800 \text{ MeV}}{Z + 1.2}. \quad (14)$$

In an electromagnetic cascade E_c defines the dividing line between shower multiplication and energy dissipation through ionization.

The transverse development of electromagnetic showers in different materials scales fairly accurately with the *Molière radius* R_M , given by²¹

$$R_M = X_0 E_s / E_c, \quad (15)$$

where $E_s = \sqrt{4\pi/\alpha} m_e c^2 = 21.2 \text{ MeV}$. The Molière radius in a material containing a weight fraction f_i of the element with critical energy E_{ci} and radiation length X_i is given by

$$\frac{1}{R_M} = \frac{1}{E_s} \sum \frac{f_i E_{ci}}{X_i}. \quad (16)$$

For photons of infinite energy, the total e^+e^- pair-production cross section is approximately

$$\sigma = \frac{7}{9} (A/X_0 N_A), \quad (17)$$

where A is the atomic weight of the material and N_A is Avogadro's number. This cross section is accurate to within a few percent down to energies as low as 1 GeV; it decreases at lower energies, as shown in the figure "Fractional Energy Loss for Electrons and Positrons in Lead." As the energy decreases a number of other processes become important, as is also shown in the figures "Contributions to the Photon Cross Section in Carbon and Lead."

(8) **Electromagnetic cascades:** When a high-energy electron or photon is incident on a thick absorber, it initiates an electromagnetic cascade as pair production and bremsstrahlung generate more electrons and photons with lower energy. The longitudinal development is governed by the high-energy part of the cascade, and therefore scales as the radiation length in the material. Electron energies eventually fall below the critical energy, and they dissipate their energy by ionization and excitation rather than by the generation of more shower particles. In describing shower behavior, it is therefore convenient to introduce the scale variables

$$\begin{aligned}
 t &= x/X_0 \\
 y &= E/E_c,
 \end{aligned} \quad (18)$$

so that distance is measured in units of radiation length and energy in units of critical energy.

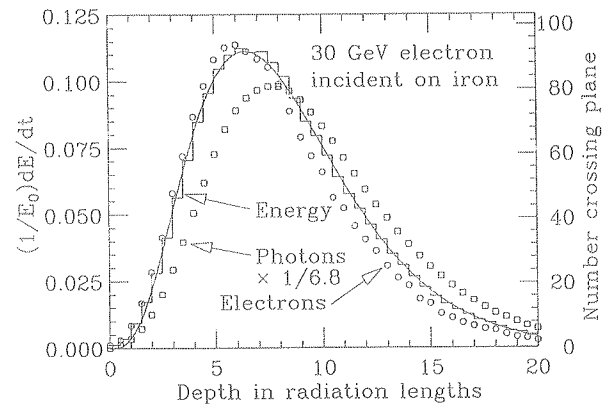


Fig. 2. An EGS4 simulation of a 30 GeV electron-induced cascade in iron. The histogram shows fractional energy deposition per radiation length, and the curve is a gamma-function fit to the distribution. Circles indicate the number of electrons with total energy greater than 1.5 MeV crossing planes at $X_0/2$ intervals (scale on right) and the squares the number of photons with $E \geq 1.5 \text{ MeV}$ crossing the planes (scaled down to have same area as the electron distribution).

Longitudinal profiles for an EGS4²² simulation of a 30 GeV electron-induced cascade in iron are shown in Fig. 2. The number of particles crossing a plane (very close to Rossi's Π function¹) is sensitive to the cutoff energy, here chosen as a total energy of 1.5 MeV for both electrons and photons. The electron number falls off more quickly than energy deposition; this is because a larger fraction of the cascade energy is carried by photons with increasing depth. Exactly what a calorimeter measures depends on the device, but it is not likely to be exactly any of the profiles shown. In gas counters it may be very close to the electron number, but in glass Čerenkov detectors and other devices with "thick" sensitive regions it is closer to the energy deposition (total track length). In such detectors the signal is proportional to the "detectable" track length T_d , which is in general less than the total track length T . Practical devices are sensitive to electrons with energy above some detection threshold E_d , and